

RESEARCH

Open Access



# An efficient multi-objective optimization approach for sensor management via multi-Bernoulli filtering

Yun Zhu<sup>1,2</sup>, Shuang Liang<sup>3\*</sup>, Guangran Xue<sup>4</sup>, Rui Yang<sup>2</sup> and Xiaojun Wu<sup>1,2\*</sup>

\*Correspondence:  
sliang@xidian.edu.cn;  
xjwu@snnu.edu.cn

<sup>1</sup> Key Laboratory of Modern Teaching Technology, Ministry of Education, Shaanxi Normal University, Xi'an, Shaanxi Province, China

<sup>2</sup> School of Computer Science, Shaanxi Normal University, Xi'an, Shaanxi Province, China

<sup>3</sup> Academy of Advanced Interdisciplinary Research, Xidian University, Xi'an, Shaanxi Province, China

<sup>4</sup> General Design Department, Beijing Institute of Radio Measurement, Beijing, China

## Abstract

Intelligent sensor management is generally required for efficient and accurate data processing when the multi-sensor system is used for multi-target tracking (MTT). However, this is theoretically and computationally challenging. To deal with this problem, we propose a novel sensor management approach based on efficient multi-objective optimization for MTT under the framework of partially observed Markov decision process. The multi-Bernoulli filter is used in conjunction with two objective functions. To simplify the multi-objective optimization problem, we use the Euclidean distance (ED) between the feasible and utopian solution vectors as a measure of the objectives and then sequentially select sensors from the candidates. For the selected sensors, we rank them according to the obtained ED measure and implement the iterated-corrector fusion scheme after the ranking. Numerical studies demonstrate the effectiveness and efficiency of our approach in multi-sensor MTT scenarios.

**Keywords:** Sensor management, Multi-sensor system, Multi-objective optimization, Multi-target tracking, Multi-Bernoulli, Random finite set

## 1 Introduction

Multi-target tracking (MTT) is one of the most significant and low-level techniques in many fields [1–7], such as military, transportation, industry, agriculture, sports, and health monitoring. For conventional tracking algorithms [8–10], MTT is usually regarded as tracking of multiple single targets. Different from those methods, finite set statistics (FISST) [11, 12] develops a unified and statistically top-down framework of multi-target filtering and makes an extensive and profound influence. Within the FISST framework, the set of targets is described as the random finite set (RFS). So far, FISST has inspired a lot of multi-target filters. For example, the probability hypothesis density (PHD) [13] and cardinalized PHD (CPHD) [14] filters were proposed by propagating moment approximations of the multi-target posterior density. The multi-Bernoulli (MB) [15] filter was developed by modeling the multi-target posterior density as MB RFSs. Examples of FISST-based algorithms also include generalized labeled MB (GLMB) [16], labeled MB (LMB) [17], and multi-scan GLMB [18] filters. These methods have been widely used in different MTT applications and provided good performances.

With the development of science and technique, the tracking system with multiple sensors has attracted lots of attention in recent years. Compared with the single-sensor system, the multi-sensor system produces much more accurate estimation by using the spatial diversity. There are three major multi-sensor system architectures, namely centralized [19–21], distributed [22–25], and decentralized [26, 27]. However, the multi-sensor MTT problem is challenging. On one hand, multi-sensor fusion is difficult because of the data association uncertainty. On the other hand, sensor management is usually necessary to collect effective measurements generated by targets and meet the communication constraints. In practical multi-target systems, there are false and miss detections. In addition, states of targets are unknown and random. These factors further increase the difficulty of sensor management.

The multi-target sensor management problem mentioned above can be solved within the FISST framework which provides a systematic manner to describe the uncertainty using multi-target probability density functions. Sensor management can be modeled as a partially observed Markov decision process (POMDP) problem [12, 28–30]. Many objective functions have been proposed within the POMDPs, mainly including information-driven and task-driven measures. The information-driven objective function quantifies the information gain obtained by the multi-target density after applying a candidate sensor management command. For example, Ristic et al. [31] proposed to use the Rényi divergence with the Bayesian multi-target filter for controlling a moving range-only sensor. Aiming at the sensor control problem, the Rényi divergence was also used with the PHD filter [32] and the MB filter [33]. In these methods, the Rényi divergence has no analytic closed-form expression, resulting in heavy computing burden. In [34], Cai et al. presented an analytical solution for the Rényi divergence of LMB RFSs by expressing the target density as a single Gaussian component. The Cauchy–Schwarz (CS) divergence [35] provides another information divergence measure. Gostar et al. [36] proposed a closed-form formula for the CS divergence of LMB RFSs and used it in solving the constrained sensor control problem. Beard et al. [37] proposed an analytical formula for the CS divergence of GLMB RFSs and demonstrated its performance in planning a sensor trajectory. Compared with the information-driven objective function, the task-driven objective function has a more direct physical meaning. In [33], Hoang et al. used the cardinality variance to define a cost function enabling an efficient sensor management. The cost function in [38] was designed as the quantitative measure of the multi-target estimation error metric. Gostar et al. [39] proposed to minimize the cardinality variance and the uncertainty within target state estimation through weight aggregation. Our recent work [40] developed the objective functions based on the different properties of tracks and demonstrated performances of the proposed objective functions using challenging MTT scenarios.

The main focus of these sensor management methods is the designing of the objective function. Whatever the objective function is, sensor management based on POMDP is in essence a global optimization problem. When it comes to the multi-sensor selection problem, the exhaustive search method is straightforward. This method first estimates the objective function for each sensor selection command and then searches for the optimal solution from all feasible solutions. When the number of candidate sensors is large, the exhaustive search method suffers from heavy computation burden (except

only one sensor is selected). To reduce the computation burden, Ma et al. [41] proposed a spatial non-maximum suppression method but needs a tuning parameter. Another approach was developed in [42] for multi-sensor control but cannot be applied to solve the sensor selection problem. Recently, we proposed a decomposed POMDP optimization approach based on the CS divergence for efficient multi-sensor selection [43]. The approach can effectively reduce the computation burden and achieved satisfactory performance. However, we only consider the optimization of a single-objective function and it is unclear how to use it to solve the multi-objective optimization (MOO) problems.

This paper studies the MOO-based multi-sensor selection problem for MTT within the POMDP framework. The major contribution of this paper is an efficient MOO approach for multi-sensor selection via MB filtering. To simplify the MOO problem, we use the Euclidean distance (ED) between the feasible solution vector and the utopian solution vector as a measure of the objectives. Instead of implementing the global combinatorial optimization, we reduce the computational complexity by sequentially selecting sensors from the candidates based on the ED measure. For the selected sensors, they send the collected measurements to the fusion center and the iterated-corrector (IC) scheme is adopted for centralized fusion. The IC scheme has simple practical implementation and has been widely used. However, the different order of sensor updates affects the result of the IC fusion. If the detection ability of the last sensor is low, the overall performance of the filter degrades. To deal with this, we first rank the selected sensors based on the obtained ED since it can reflect the detection ability of the sensor. Then, the IC update is applied in order of the ranking. Simulation results obtained from challenging MTT scenarios demonstrate that the proposed method works significantly faster than the exhaustive search scheme and provides similar tracking accuracy in terms of the optimal sub-pattern assignment (OSPA) error.

The paper is organized as follows. In Sect. 2, we briefly introduce the POMDP framework, the multi-target Bayes filter, and the MB filter. In Sect. 3, the objective functions, the efficient MOO, and the detailed implementation of the proposed approach are presented. Section 4 presents numerical studies. In Sect. 5, we derive conclusions of the paper.

## 2 Background

### 2.1 Partially observable Markov decision process

For MTT in multi-sensor systems, sensor selection is generally required to collect effective measurements generated by targets and meet the communication constraints. This problem is challenging because the selection commands is made before the current multi-target state is observed. The POMDP framework [12] provides a statistically unified solution to such problems. At time  $k$ , the POMDP problem is modeled as

$$\Psi = \{X_k, \mathbb{S}, f_{k|k-1}(X_k|X_{k-1}), g_k(Z_k|X_k), \vartheta(A_k)\}, \quad (1)$$

where  $X_k$  is the multi-target state,  $\mathbb{S}$  denotes the set of sensor selection commands,  $f_{k|k-1}(X_k|X_{k-1})$  is the multi-target transition function from  $X_{k-1}$  to  $X_k$ ,  $g_k(Z_k|X_k)$  is the multi-target likelihood, and  $\vartheta(A_k)$  is the objective function measuring a cost or reward when the sensor selection command  $A_k$  is applied.

The objective function is an important criterion to determine the performance of sensor selection. Sensor selection can be regarded as a combinatorial optimization problem finding the optimal combination of sensors that minimizes or maximizes the objective function, as follows:

$$A_k^* = \underset{A_k \subseteq \mathbb{S}}{\operatorname{argmin}} / \underset{A_k \subseteq \mathbb{S}}{\operatorname{argmax}} \{E_{Z_k(A_k)}[\vartheta(A_k)]\}. \tag{2}$$

Note that the myopic policy with the multi-target state transiting from  $X_{k-1}$  to  $X_k$  is considered, whereas the POMDP can solve  $p$ -step future decision problems.

### 2.2 Multi-target Bayes filter

An RFS is a finite-set-valued random variable that the set cardinality is random and each element in the set is also random. At time  $k$ , we assume that the target states are  $x_{k,1}, x_{k,2}, \dots, x_{k,N_k}$  and the measurements are  $z_{k,1}, z_{k,2}, \dots, z_{k,M_k}$ , where  $N_k$  and  $M_k$  denote the number of targets and the number of measurements, respectively. In the RFS approach, the finite sets of targets and measurements are denoted as the multi-target state  $X_k$  and multi-target measurement  $Z_k$ , respectively

$$X_k = \{x_{k,1}, \dots, x_{k,N_k}\} \in \mathcal{F}(\mathcal{X}), \tag{3}$$

$$Z_k = \{z_{k,1}, \dots, z_{k,M_k}\} \in \mathcal{F}(\mathcal{Z}), \tag{4}$$

where  $\mathcal{F}(\mathcal{X})$  and  $\mathcal{F}(\mathcal{Z})$  denote the multi-target state space and multi-target measurement space, respectively. Based on the RFS assumptions, recursion of the multi-target state is modeled as the following Bayes filtering problem.

At time  $k$ ,  $\pi_k(X_k|Z_{1:k})$  is used to denote the multi-target density with  $Z_{1:k} = (Z_1, \dots, Z_k)$ . The multi-target Bayes filter propagates  $\pi_k(X_k|Z_{1:k})$  using the following formulas

$$\pi_{k|k-1}(X_k|Z_{1:k-1}) = \int f_{k|k-1}(X_k|X)\pi_{k-1}(X|Z_{1:k-1})\delta X, \tag{5}$$

$$\pi_k(X_k|Z_{1:k}) = \frac{g_k(Z_k|X_k)\pi_{k|k-1}(X_k|Z_{1:k-1})}{\int g_k(Z_k|X)\pi_{k|k-1}(X|Z_{1:k-1})\delta X}, \tag{6}$$

where the integrals in Eqs. (5), (6) are set integrals. The set integral for a multi-target density function  $f(Y)$  is defined as

$$\int f(Y)\delta Y = \sum_{i=0}^{\infty} \frac{1}{i!} \int f(\{y_1, \dots, y_i\})dy_1 \dots dy_i \tag{7}$$

$$= f(\emptyset) + \sum_{i=1}^{\infty} \frac{1}{i!} \int f(\{y_1, \dots, y_i\})dy_1 \dots dy_i \tag{8}$$

$$\stackrel{\text{def.}}{=} f(\emptyset) + \sum_{i=1}^{\infty} \int f_i(y_1, \dots, y_i)dy_1 \dots dy_i \tag{9}$$

The set integral has no analytic solution and the multi-target Bayes filter is computationally expensive. Therefore, several RFS-based filters have been proposed as its approximations.

### 2.3 Multi-Bernoulli filter

The MB filter is an approximation of the multi-target Bayes filter. For a Bernoulli RFS  $X$  on  $\mathcal{X}$ , it either contains a single element distributed with the probability density  $p$  or is an empty set. Assuming that the probability of being a singleton is  $r$ , the probability density of the Bernoulli RFS  $X$  is

$$\pi(X) = \begin{cases} 1 - r & X = \emptyset, \\ rp(x) & X = \{x\} \end{cases} \tag{10}$$

The MB RFS containing  $M$  independent components is defined as  $X = \cup_{i=1}^M X^{(i)}$ . If the probability of existence and the probability density for  $X^{(i)}$  are  $r^{(i)}$  and  $p^{(i)}$ , respectively, the probability density  $\pi$  of the MB RFS is

$$\pi(\{x_1, \dots, x_n\}) = \pi(\emptyset) \sum_{1 \leq i_1 \neq \dots \neq i_n \leq M} \prod_{j=1}^n \frac{r^{(i_j)} p^{(i_j)}(x_j)}{1 - r^{(i_j)}} \tag{11}$$

where  $\pi(\emptyset) = \prod_{j=1}^M (1 - r^{(j)})$  denotes the probability that all components are empty. For simplicity, the MB RFS is denoted as  $\pi = \{(r^{(i)}, p^{(i)})\}_{i=1}^M$ .

If the multi-target density at time  $k - 1$  is described as an MB RFS  $\pi_{k-1} = \{(r_{k-1}^{(i)}, p_{k-1}^{(i)})\}_{i=1}^{M_{k-1}}$ , the predicted multi-target density at time  $k$  obtained by the MB filter is also an MB RFS and is given as

$$\pi_{k|k-1} = \left\{ \left( r_{p,k|k-1}^{(i)}, p_{p,k|k-1}^{(i)} \right) \right\}_{i=1}^{M_{k-1}} \cup \left\{ \left( r_{\Gamma,k}^{(i)}, p_{\Gamma,k}^{(i)} \right) \right\}_{i=1}^{M_{\Gamma,k}}, \tag{12}$$

where  $\{(r_{p,k|k-1}^{(i)}, p_{p,k|k-1}^{(i)})\}_{i=1}^{M_{k-1}}$  and  $\{(r_{\Gamma,k}^{(i)}, p_{\Gamma,k}^{(i)})\}_{i=1}^{M_{\Gamma,k}}$  denote the MB RFS for the surviving and birth targets, respectively. Parameters of  $\{(r_{p,k|k-1}^{(i)}, p_{p,k|k-1}^{(i)})\}_{i=1}^{M_{k-1}}$  are computed as follows

$$r_{p,k|k-1}^{(i)} = r_{k-1}^{(i)} \langle p_{k-1}^{(i)}, p_{S,k} \rangle \tag{13}$$

$$p_{p,k|k-1}^{(i)}(x) = \frac{\langle f_{k|k-1}(x|\cdot), p_{k-1}^{(i)} p_{S,k} \rangle}{\langle p_{k-1}^{(i)}, p_{S,k} \rangle}, \tag{14}$$

where  $f_{k|k-1}(x|\cdot)$  is the single-target transition density,  $p_{S,k}$  is the survival probability, and  $\langle f, g \rangle \triangleq \int f(x)g(x)dx$  is the standard inner product notation.

If the predicted density is an MB RFS  $\pi_{k|k-1} = \{(r_{k|k-1}^{(i)}, p_{k|k-1}^{(i)})\}_{i=1}^{M_{k|k-1}}$ , the posterior density at time  $k$  can also be described as an MB RFS

$$\pi_k \approx \left\{ \left( r_{L,k}^{(i)}, p_{L,k}^{(i)} \right) \right\}_{i=1}^{M_{k|k-1}} \cup \left\{ \left( r_{U,k}(z), p_{U,k}(\cdot; z) \right) \right\} \quad z \in Z_k \tag{15}$$

where  $\left\{ \left( r_{L,k}^{(i)}, p_{L,k}^{(i)} \right) \right\}_{i=1}^{M_{k|k-1}}$  and  $\{(r_{U,k}(z), p_{U,k}(\cdot; z))\}$  are the MB RFSs for the legacy tracks and the measurement-updated tracks, respectively. Parameters of the posterior density  $\pi_k$  are computed as follows

$$r_{L,k}^{(i)} = r_{k|k-1}^{(i)} \frac{1 - \langle p_{k|k-1}^{(i)}, p_{D,k} \rangle}{1 - r_{k|k-1}^{(i)} \langle p_{k|k-1}^{(i)}, p_{D,k} \rangle} \tag{16}$$

$$p_{L,k}^{(i)}(x) = p_{k|k-1}^{(i)}(x) \frac{1 - p_{D,k}(x)}{1 - \langle p_{k|k-1}^{(i)}, p_{D,k} \rangle} \tag{17}$$

$$r_{U,k}(z) = \frac{\sum_{i=1}^{M_{k|k-1}} \frac{r_{k|k-1}^{(i)} (1 - r_{k|k-1}^{(i)}) \langle p_{k|k-1}^{(i)}, \psi_{k,z} \rangle}{(1 - r_{k|k-1}^{(i)} \langle p_{k|k-1}^{(i)}, p_{D,z} \rangle)^2}}{\kappa_k(z) + \sum_{i=1}^{M_{k|k-1}} \frac{r_{k|k-1}^{(i)} \langle p_{k|k-1}^{(i)}, \psi_{k,z} \rangle}{1 - r_{k|k-1}^{(i)} \langle p_{k|k-1}^{(i)}, p_{D,z} \rangle}} \tag{18}$$

$$p_{U,k}(x; z) = \frac{\sum_{i=1}^{M_{k|k-1}} \frac{r_{k|k-1}^{(i)} p_{k|k-1}^{(i)}(x) \psi_{k,z}(x)}{1 - r_{k|k-1}^{(i)} \langle p_{k|k-1}^{(i)}, p_{D,z} \rangle}}{\sum_{i=1}^{M_{k|k-1}} \frac{r_{k|k-1}^{(i)} \langle p_{k|k-1}^{(i)}, \psi_{k,z} \rangle}{1 - r_{k|k-1}^{(i)} \langle p_{k|k-1}^{(i)}, p_{D,z} \rangle}} \tag{19}$$

$$\psi_{k,z}(x) = g_k(z|x) p_{D,k}(x) \tag{20}$$

where  $p_{D,k}(x)$  is the detection probability,  $g_k(\cdot|x)$  is the single-target likelihood function, and  $\kappa_k(\cdot)$  is the clutter intensity.

### 3 Methods

#### 3.1 Objective functions

The posterior multi-target density (15) of the MB filter consists of legacy and measurement-updated tracks which have different theoretical and physical meanings. In our work [40], it is proved that considering these two kinds of tracks separately enables an effective sensor management strategy. Therefore, the objective functions used in the proposed POMDP model are as follows [40],

$$\sigma_{L,k|k}^2(A_k) = \sum_{i=1}^{M_{k|k-1}} r_{L,k}^{(i)}(Z_k(A_k)) \left( 1 - r_{L,k}^{(i)}(Z_k(A_k)) \right) \tag{21}$$

$$N_{U,k|k}(A_k) = \sum_{Z_k(A_k) \in Z_k(s)} r_{U,k}(Z_k(A_k)) \tag{22}$$

where  $Z_k(A_k)$  denotes the set of measurements obtained from  $A_k$ , and  $\sigma_{L,k|k}^2(A_k)$  and  $N_{U,k|k}(A_k)$  are the cardinality variance of legacy tracks and the mean cardinality of measurement-updated tracks, respectively. When  $\sigma_{L,k|k}^2(A_k)$  is used as the cost function, sensor management aims at reducing the uncertainty for the number of legacy tracks,

whereas if we use  $N_{U,k|k}(A_k)$  as the reward function, sensor management aims to maximize the number of detected targets.

### 3.2 Efficient multi-objective optimization

Although the objective functions (21) and (22) are considered simultaneously in [40], only one sensor is selected at each time step, which makes the problem simple. In this paper, we consider a more general problem and study the selection of multiple sensors. At time  $k$ , the MOO-based sensor management is described mathematically as

$$\begin{aligned} &\text{Minimize } F(A_k) = [\vartheta_1(A_k), \vartheta_2(A_k)]^T, \\ &\text{subject to } A_k \subseteq \mathbb{S}, \end{aligned} \tag{23}$$

where  $\vartheta_1(A_k) = -N_{U,k|k}(A_k)$ ,  $\vartheta_2(A_k) = \sigma_{L,k|k}^2(A_k)$ , and  $F(A_k)$  is the objective vector. Note that computation of the multi-target posterior density and the objective function depends on the future measurement set. However, this is unpractical because the true measurements kept unknown before applying the sensor management command. In theory, it is necessary to use all possible measurement sets to compute objective functions, requiring a large amount of computation. We use the predicted ideal measurement set (PIMS) approach proposed in [44] to reduce the computing load. In (23), we negate  $N_{U,k|k}(A_k)$  and translate its maximization into minimization to formulate a general optimization. Finding the global optimum of (23) is NP-hard. To reduce the computation burden, we propose a novel efficient MOO approach for sensor management. At each time step, we assume that  $P$  sensors are selected from the complete set. Motivated by the decomposed POMDP approach proposed in [43], the MOO problem is decomposed into a set of simple MOO subproblems for individual sensors to avoid the global combinatorial optimization. Instead of searching for the global optimal solution, sensors are selected sequentially from candidates. The mathematical description of the decomposed MOO problem is described as follows:

$$\begin{aligned} &\text{Minimize } F(A_k^{(j)}) = [\vartheta_1(A_k^{(j)}), \vartheta_2(A_k^{(j)})]^T, \\ &\text{subject to; } \begin{cases} A_k^{(j)} \in \mathbb{S} \text{ and } |A_k^{(j)}| = 1, \\ j \in \{1, \dots, P\} \end{cases} \end{aligned} \tag{24}$$

and

$$A_k^* = \cup_{j=1}^P A_k^{(j)*}, \tag{25}$$

where  $A_k^{(j)*}$  is the  $j$ th selected sensor,  $A_k^*$  is the resulting selection command, and  $\mathbb{S}$  is the set of remaining sensors.

To solve (24), a conventional approach is to convert the MOO into the single-objective optimization by weighting objective functions. This approach has major drawbacks. For example, it is required to estimate the importance of each objective function. We take a simple strategy and use the ED between the feasible solution vector and the utopian solution vector as a measure of the objectives. The utopia solution vector of the multi-objective problem is defined as

$$F^* = [\vartheta_1^*, \vartheta_2^*]^T, \tag{26}$$

where  $\vartheta_1^*$  and  $\vartheta_2^*$  are the minima of objectives  $\vartheta_1(A_k^{(j)})$  and  $\vartheta_2(A_k^{(j)})$ , respectively. The ED of a feasible solution vector  $F(A_k^{(j)}) = [\vartheta_1(A_k^{(j)}), \vartheta_2(A_k^{(j)})]^T$  from the utopia solution vector can be determined as follows

$$d_{\text{Euc}}[F(A_k^{(j)}), F^*] = \sqrt{[\vartheta_1(A_k^{(j)}) - \vartheta_1^*]^2 + [\vartheta_2(A_k^{(j)}) - \vartheta_2^*]^2}. \tag{27}$$

If the ED between a feasible solution vector and the utopia solution vector is smaller, then the solution is more preferable for a decision maker. Therefore, the solution for the MOO problem is given by

$$A_k^{(j)*} = \underset{A_k^{(j)} \in \mathbb{S}}{\operatorname{argmin}} \{d_{\text{Euc}}[F(A_k^{(j)}), F^*]\}. \tag{28}$$

Assuming that there are ten candidate sensors in the multi-sensor system and three sensors are selected, an illustrative example of the proposed decomposed MOO approach is shown in Fig. 1, where  $F^j$  is the objective vector of the candidate sensor  $j$  and  $j = 1, 2, \dots, 10$ . In this illustration, it is straightforward that sensor 3, sensor 6, and sensor 9 will be selected using (28).

### 3.3 Implementation

The IC scheme is used for data fusion of the selected sensors. Although the IC approach has no rigorous mathematical derivation, it is easy to implement and has been widely used. Algorithms 1 shows the pseudo-codes of the multi-sensor MB filter with the IC fusion scheme.

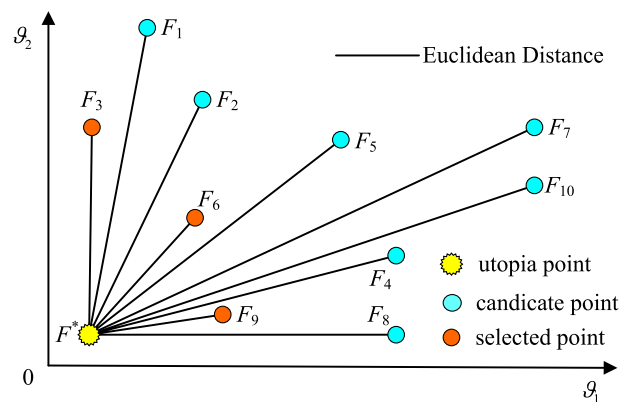


Fig. 1 Illustration of the proposed decomposed MOO approach

---

**Algorithm 1** Multi-sensor MB filter with IC fusion.

---

**INPUT:** → The posterior MB RFS  $\pi_{k-1} = \{r_{k-1}^{(i)}, p_{k-1}^{(i)}\}_{i=1}^{M_{k-1}}$  from previous time  $k - 1$   
**OUTPUT:** → The posterior MB RFS  $\pi_k = \{r_k^{(i)}, p_k^{(i)}\}_{i=1}^{M_k}$  at current time  $k$

- 1: **for**  $j = 1, \dots, P$  **do**
- 2:     **if**  $j = 1$  **then**
- 3:         Predict the MB RFS  $\pi_{k|k-1}^j = \{r_{k|k-1}^{(i)}, p_{k|k-1}^{(i)}\}_{i=1}^{M_{k|k-1}}$  using (12)-(14)
- 4:         **else**
- 5:             Pseudo-predict  $\pi_{k|k-1}^j = \pi_k^j$
- 6:         **end if**
- 7:         Update the MB RFS  $\pi_{k|k-1}^j$  to obtain  $\pi_k^j = \{r_k^{(i)}, p_k^{(i)}\}_{i=1}^{M_k}$  using (15)-(20)
- 8:     **end for**
- 9: Obtain the posterior MB RFS  $\pi_k = \pi_k^j$

---

When the detection performances of the sensors are different, the result of the IC scheme is influenced by the order of the sensor updates. If the detection ability of the last sensor is low, the overall performance of the filter degrades. A solution to this problem is to rank the sensors according to their ability to detect the target and then implement the IC fusion based on the ranking result [43]. In this paper, sensors are ranked according to ED obtained in (27), as follows

$$\text{ranked}(A_k) = \text{sort}\{d_{\text{Euc}}[A_k, F^*], 'descend'\}, \tag{29}$$

where  $d_{\text{Euc}}[A_k, F^*] = \{d_{\text{Euc}}[F(A_k^{(j)}), F^*], \dots, d_{\text{Euc}}[F(A_k^{(j)}), F^*]\}$  and the operator  $\text{sort}\{Y, 'descend'\}$  indicates sorting the elements of vector  $Y$  from largest to smallest and obtaining the sort index. Using this method, the ranking of the selected sensors in Fig. 1 is: sensor 9, sensor 6, and sensor 3.

An overall schematic diagram of the proposed MB MTT with sensor management is illustrated in Fig. 2. To deal with the nonlinear target dynamics and measurement model, the MB filter is implemented using the sequential Monte Carlo (SMC) method. At time  $k$ , the probability density  $p_k^i$  for the  $i$ th Bernoulli component is approximated as follows

$$p_k^{(i)} = \sum_{j=1}^{L_k^{(i)}} w^{(i,j)} \delta_{x^{(i,j)}}(x) \tag{30}$$

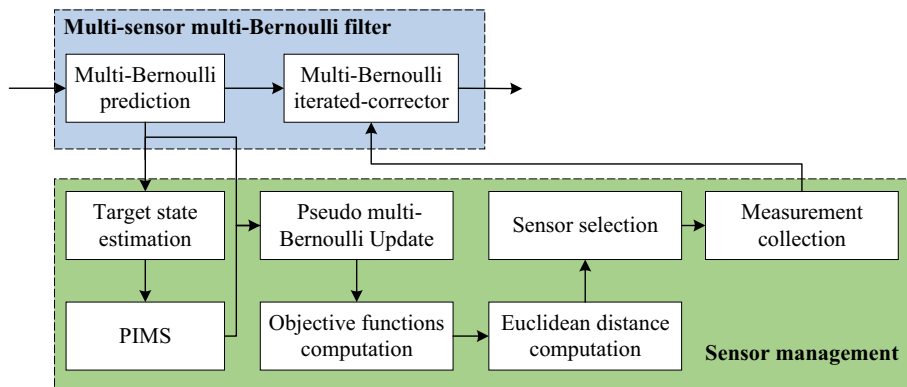


**Fig. 2** Schematic diagram of the proposed MB MTT with sensor management

where  $L_k^{(i)}$  is the number of particles,  $\delta_a(x)$  is the Dirac delta function, and  $w^{(ij)}$  is the normalized weight corresponding to the  $j$ th particle. To improve the computational efficiency, the Bernoulli components whose existence probabilities below the threshold  $T$  are pruned. Besides, the number of particles for the remaining component is limited to the maximum  $L_{\max}$  and minimum  $L_{\min}$ . Refer to [15] for a detailed SMC implementation of the MB filter.

#### 4 Results and discussion

In this section, the performance of the proposed efficient MOO with improved IC (EMO-IIC) method is demonstrated using two challenging multi-sensor MTT scenarios. There is one transmitter and ten receivers located in the surveillance area, and the structure of the multi-sensor system is the same as that in [40, 43, 45]. The sampling interval is fixed to  $T_s = 10$  s. The detection probability of a receiver  $j$  located at  $r^j$  for a target with position  $p$  is modeled as follows:

$$p_D(r^j, p) = \begin{cases} 1 & \text{if } \|r^j - p\| \leq R_0, \\ \max\{0, 1 - \eta(\|r^j - p\| - R_0)\} & \text{otherwise,} \end{cases} \tag{31}$$

where  $\|r^j - p\|$  denotes the distance between receiver  $j$  and the target,  $\eta = 1e - 4$ , and  $R_0 = 5000$  m. The detection probability decreases rapidly as  $\|r^j - p\|$  increases.

For targets being tracked, a nearly constant turn model is considered. The target state is  $x_k = [\tilde{x}_k^T, \omega_k]^T$  in which  $\tilde{x}_k = [p_{x,k}, \dot{p}_{x,k}, p_{y,k}, \dot{p}_{y,k}]^T$  and  $\omega_k$  is the turn rate. The transition of the target state is modeled as

$$\tilde{x}_k = F(\omega)\tilde{x}_{k-1} + Gw_{k-1}, \tag{32}$$

$$w_k = w_{k-1} + \Delta u_{k-1}, \tag{33}$$

where

$$F(\omega) = \begin{bmatrix} 1 & \frac{\sin \omega T_s}{\omega} & 0 & -\frac{1 - \cos \omega T_s}{\omega} \\ 0 & \cos \omega T_s & 0 & -\sin \omega T_s \\ 0 & \frac{1 - \cos \omega T_s}{\omega} & 1 & \frac{\sin \omega T_s}{\omega} \\ 0 & \sin \omega T_s & 0 & \cos \omega T_s \end{bmatrix}, \tag{34}$$

$$G = \begin{bmatrix} \frac{T_s^2}{2} & 0 \\ T_s & 0 \\ 0 & \frac{T_s^2}{2} \\ 0 & T_s \end{bmatrix}, \tag{35}$$

$w_{k-1} \sim \mathcal{N}(0; 0, \sigma_w^2 I_2)$  with  $\sigma_w = 0.01$  m/s<sup>2</sup>, and  $u_{k-1} \sim \mathcal{N}(0; 0, \sigma_u^2 I_2)$  with  $\sigma_u = 0.0001$  rad/s. If a target is detected by a receiver at time  $k$ , then the receiver will report a bearing and bistatic range measurement vector as follows:

$$z_k^j = \begin{bmatrix} \varphi^j \\ \rho^j \end{bmatrix} = \begin{bmatrix} \arctan \left( \frac{p_{y,k} - r_y^j}{p_{x,k} - r_x^j} \right) \\ \|p_k - r^j\| + \|p_k - t\| \end{bmatrix} + \mathbf{e}_k^j, \tag{36}$$

where  $\epsilon_k^j \sim \mathcal{N}(0; 0, R_k^j)$  with  $R_k^j = \text{diag}([\sigma_\varphi^2, \sigma_\rho^2])$ ,  $\sigma_\varphi = \pi/180$  rad,  $\sigma_\rho = 5$  m,  $t = [t_x, t_y]^T$  is the transmitter location, and  $p_k = [p_{x,k}, p_{y,k}]^T$  denotes the target position. With the moving of targets,  $P$  receivers are adaptively selected at each time step. The OSPA error distance [46] is used to measure the tracking accuracy, which is widely used by the RFS-based methods. The average results are obtained over 50 independent Monte Carlo (MC) simulations.

### 4.1 Experiment 1

In the first scenario, a total of three targets appear in the surveillance area. The birth process of the MB filter is modeled as  $\left\{ \left( r_\Gamma^{(i)}, p_\Gamma^{(i)} \right) \right\}_{i=1}^3$  where  $r_\Gamma^{(1)} = r_\Gamma^{(2)} = r_\Gamma^{(3)} = 0.02$ ,  $p_\Gamma^{(i)} = \mathcal{N}(x; m_\Gamma^{(i)}, P_\Gamma^{(i)})$ ,  $m_\Gamma^{(1)} = [1500, 0, -8250, 0, 0]^T$ ,  $m_\Gamma^{(2)} = [0, 0, -6000, 0, 0]^T$ ,  $m_\Gamma^{(3)} = [1500, 0, -5000, 0, 0]^T$ , and  $P_\Gamma^{(1)} = P_\Gamma^{(2)} = P_\Gamma^{(3)} = \text{diag}([10, 2, 10, 2, (\pi/18000)]^T)^2$ . The units are meters for  $x$  and  $y$  and meters per second for  $\dot{x}$  and  $\dot{y}$ . For each hypothesized track, we use  $L_{\min} = 300$  and  $L_{\max} = 1000$  particles. The hypothesized tracks with the existence probabilities below  $T = 1e - 3$  are pruned. The probability of survival is  $p_S = 0.99$ . When  $P = 3$  receivers are selected at each time step, the position estimates of the proposed EMO-IIC approach for a single MC run are shown in Fig. 3. It can be observed that the EMO-IIC approach is able to detect the births of targets and can well estimate the target positions.

In order to analyze the performance EMO-IIC approach, the heuristic random selection approach, the exhaustive search scheme, and the EMO-IC approach are used as the comparative algorithms. In the heuristic random selection approach, the probability for each candidate sensor to be selected is equal. In the exhaustive search scheme, the ED in (27) is estimated for every possible combination of sensors and then search for the optimal solution. The EMO-IC approach is the one that uses the proposed efficient MOO sensor management and uses the standard IC fusion scheme without ranking of sensors. The average OSPA distance errors (with  $p = 1$ ,  $c = 300$

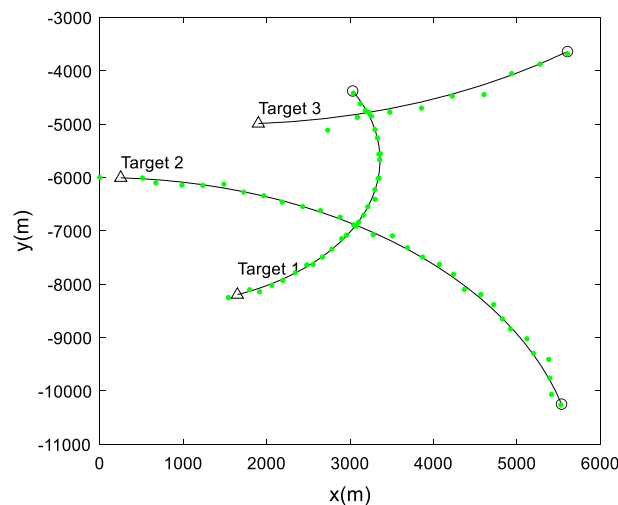


**Fig. 3** True and estimated positions in Experiment 1. The black solid line indicates the real trajectory of the target, and the green dot denotes the estimated target positions

m) for different sensor management approaches with  $P = 3$  are given in Fig. 4. Compared with other approaches, the performance of the random selection approach is worse because it does not use any technical sensor management strategy. In the considered challenging scenario, the detection abilities of different receivers vary greatly with the moving of targets. In this case, different rankings of receivers result in different tracking results. As can be observed from Fig. 4, the performance of the EMO-IIC approach is better than that of the EMO-IC approach and even comparable with the exhaustive search scheme.

In terms of the computational efficiency, the average computing time for a complete MC run of the random selection approach, the EMO-IIC approach, and the exhaustive search scheme is 2.05 s, 9.87 s, and 1932.92 s, respectively. Without using any technical sensor management strategy, the random selection approach costs less computation time than other approaches. The EMO-IIC approach achieves a satisfactory computational efficiency and is about 195.84 times faster than the exhaustive search method.

#### 4.2 Experiment 2

In this scenario, the number of targets being tracked is increased into five. The birth process of the MB filter is modeled as  $\left\{ \left( r_{\Gamma}^{(i)}, p_{\Gamma}^{(i)} \right) \right\}_{i=1}^3$  where  $r_{\Gamma}^{(1)} = r_{\Gamma}^{(2)} = r_{\Gamma}^{(3)} = 0.02$ ,  $p_{\Gamma}^{(i)} = \mathcal{N}(x; m_{\Gamma}^{(i)}, P_{\Gamma}^{(i)})$ ,  $m_{\Gamma}^{(1)} = [1500, 0, 1000, 0, 0]^T$ ,  $m_{\Gamma}^{(2)} = [0, 0, -7000, 0, 0]^T$ ,  $m_{\Gamma}^{(3)} = [1500, 0, -5000, 0, 0]^T$ , and  $P_{\Gamma}^{(1)} = P_{\Gamma}^{(2)} = P_{\Gamma}^{(3)} = \text{diag}([10, 2, 10, 2, (\pi/18000)]^T)^2$ . The hypothesized tracks with the existence probabilities below  $T = 1e - 5$  are pruned. Other parameters used in the MB filter are the same with those in Experiment 1. When  $P = 3$  receivers are selected at each time step, the position estimates of the proposed EMO-IIC approach for a single MC run are shown in Fig. 5. It can be observed that the position estimates of the EMO-IIC approach are close to the true target trajectories.

The average OSPA distance errors (with  $p = 1, c = 300$  m) are shown in Fig. 6. The exhaustive search scheme is not considered in this scenario since its computing

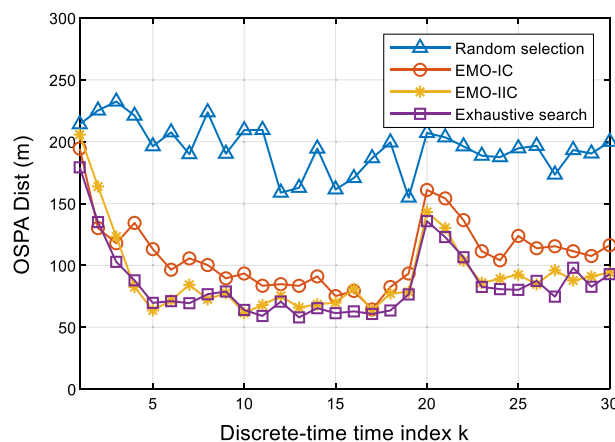
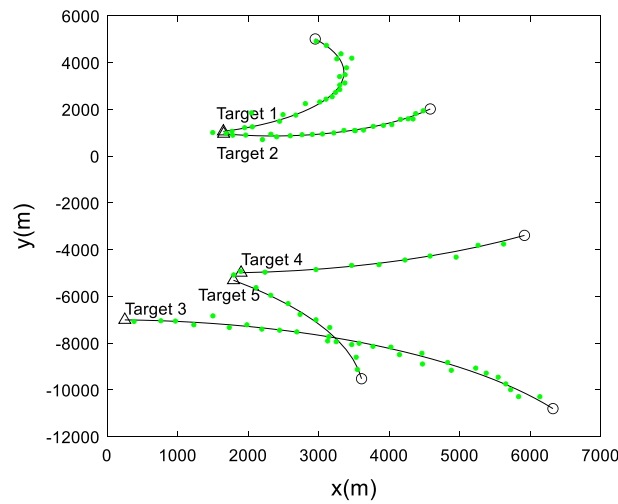
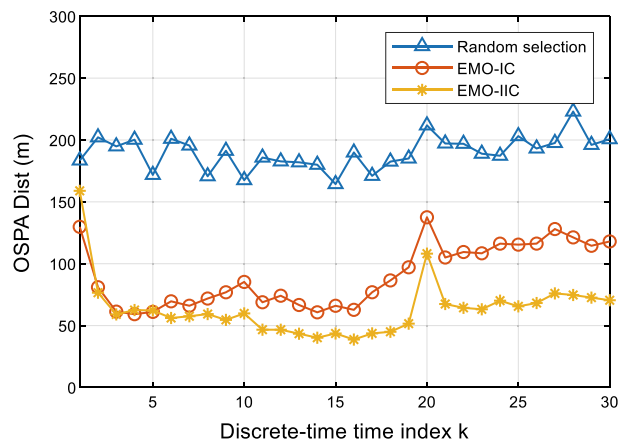


Fig. 4 Average OSPA distances in Experiment 1



**Fig. 5** True and estimated positions in Experiment 2. The black solid line indicates the real trajectory of the target, and the green dot denotes the estimated target positions



**Fig. 6** Average OSPA distances in Experiment 2

burden is overload. It can be observed that the EMO-IIC approach achieves the minimum tracking error in Fig. 6, indicating that the proposed improved IC method also works well in this scenario. The average computing time for a complete MC run of the random selection approach and the EMO-IIC approach is 3.49 s and 20.830 s, respectively. The proposed method still has a satisfactory computational efficiency.

### 5 Conclusion

An MOO-based sensor management approach for MTT in the multi-sensor system has been proposed in this paper. To avoid the global combinatorial optimization, the complex MOO problem is decomposed into a set of simple MOO subproblems for individual sensors. For the selected sensors, an improved IC scheme is used to improve performances of the multi-sensor fusion. Simulation results obtained from two challenging MTT with sensor management scenarios showed the superior tracking accuracy of the proposed approach. It is also demonstrated that the proposed approach works

much more efficiently than the exhaustive search scheme. Future work will investigate the efficient sensor management solutions for distributed and decentralized fusion architectures.

#### Abbreviations

MTT	Multi-target tracking
FISST	Finite set statistics
RFS	Random finite set
PHD	Probability hypothesis density
CPHD	Cardinalized probability hypothesis density
MB	Multi-Bernoulli
GLMB	Generalized labeled multi-Bernoulli
POMDP	Partially observed Markov decision process
CS	Cauchy–Schwarz
OSPA	Optimal sub-pattern assignment
PIMS	Predicted ideal measurement set
MOO	Multi-objective optimization
IC	Iterated-corrector
ED	Euclidean distance
SMC	Sequential Monte Carlo
EMO-IC	Efficient multi-objective optimization with improved iterated-corrector
EMO-IC	Efficient multi-objective optimization with iterated-corrector
MC	Monte Carlo

#### Acknowledgements

Not applicable.

#### Author contributions

Yun Zhu developed the algorithm, conducted the experiments, and participated in writing the paper. Shuang Liang contributed to the theoretical analysis of the algorithm. Guangran Xue and Rui Yang participated in writing the paper. Xiaojun Wu supervised the overall work and reviewed the paper. All authors read and approved the final manuscript.

#### Funding

This work was supported in part by the National Natural Science Foundation of China under grant number 62007022, the Natural Science Foundation of Shaanxi Province under grant number 2021JQ-209, and the Fundamental Research Funds for the Central Universities under grant number GK202103082 and XJS212210.

#### Availability of data and materials

In this work, we have used the free RFS MATLAB code provided by Prof. Ba-Ngu Vo and Prof. Ba-Tuong Vo at <http://ba-tuong.vo-au.com/codes.html>.

#### Declarations

##### Ethics approval and consent to participate

Not applicable.

##### Consent for publication

Not applicable.

##### Competing interests

The authors declare that they have no competing interests.

Received: 27 March 2022 Accepted: 30 May 2022

Published online: 15 July 2022

#### References

1. J. Yan, W. Pu, S. Zhou, H. Liu, Z. Bao, Collaborative detection and power allocation framework for target tracking in multiple radar system. *Inf. Fusion* **55**, 173–183 (2020)
2. J. Yan, W. Pu, S. Zhou, H. Liu, M.S. Greco, Optimal resource allocation for asynchronous multiple targets tracking in heterogeneous radar networks. *IEEE Trans. Signal Process.* **68**, 4055–4068 (2020)
3. J. Yan, J. Dai, W. Pu, H. Liu, M. Greco, Target capacity based resource optimization for multiple target tracking in radar network. *IEEE Trans. Signal Process.* **69**, 2410–2421 (2021)
4. J. Zhou, T. Li, X. Wang, L. Zheng, Target tracking with equality/inequality constraints based on trajectory function of time. *IEEE Signal Process. Lett.* **28**, 1330–1334 (2021)
5. S. Liang, Y. Zhu, H. Li, Evolutionary optimization based set joint integrated probabilistic data association filter. *Electronics* **11**(4), 1–15 (2022)

6. Y. Zhu, S. Liang, X. Wu, H. Yang, A random finite set based joint probabilistic data association filter with non-homogeneous Markov chain. *Front. Inf. Technol. Electron. Eng.* **22**(8), 1114–1126 (2021)
7. Y. Zhu, H. Li, Y. Zhang, X. Wu, Receiver selection for multi-target tracking in multi-static Doppler radar systems. *EURASIP J. Adv. Sig. Process.* **118**, 1–16 (2021)
8. D. Reid, An algorithm for tracking multiple targets. *IEEE Trans. Autom. Control* **24**(6), 843–854 (1979)
9. T. Kurien, Issues in the design of practical multitarget tracking algorithms, in *Multitarget-Multisensor Tracking: Advanced Applications*, ed. by Y. Bar-Shalom (Artech House, Norwood, 1990), pp. 43–83
10. T. Fortmann, Y. Bar-Shalom, M. Scheffe, Sonar tracking of multiple targets using joint probabilistic data association. *IEEE J. Ocean. Eng.* **8**(3), 173–184 (1983)
11. R.P. Mahler, *Statistical Multisource-Multitarget Information Fusion* (Artech House, Norwood, 2007)
12. R.P. Mahler, *Advances in Statistical Multisource-Multitarget Information Fusion* (Artech House, Norwood, 2014)
13. R. Mahler, Multitarget Bayes filtering via first-order multitarget moments. *IEEE Trans. Aerosp. Electron. Sys.* **39**(4), 1152–1178 (2003)
14. R. Mahler, PHD filters of higher order in target number. *IEEE Trans. Aerosp. Electron. Sys.* **43**(4), 1523–1543 (2007)
15. B.-T. Vo, B.-N. Vo, A. Cantoni, The cardinality balanced multi-target multi-Bernoulli filter and its implementations. *IEEE Trans. Signal Process.* **57**(2), 409–423 (2009)
16. B.-N. Vo, B.-T. Vo, D. Phung, Labeled random finite sets and the Bayes multi-target tracking filter. *IEEE Trans. Signal Process.* **62**(24), 6554–6567 (2014)
17. S. Reuter, B.-T. Vo, B.-N. Vo, K. Dietmayer, The labeled multi-bernoulli filter. *IEEE Trans. Signal Process.* **62**(12), 3246–3260 (2014)
18. B.-N. Vo, B.-T. Vo, A multi-scan labeled random finite set model for multi-object state estimation. *IEEE Trans. Signal Process.* **67**(19), 4948–4963 (2019)
19. A.K. Gostar, T. Rathnayake, R. Tennakoon, A. Bab-Hadiashar, G. Battistelli, L. Chisci, R. Hoseinnezhad, Cooperative sensor fusion in centralized sensor networks using Cauchy-Schwarz divergence. *Signal Process.* **167**, 107278 (2020)
20. A.K. Gostar, T. Rathnayake, R. Tennakoon, A. Bab-Hadiashar, G. Battistelli, L. Chisci, R. Hoseinnezhad, Centralized cooperative sensor fusion for dynamic sensor network with limited field-of-view via labeled multi-Bernoulli filter. *IEEE Trans. Signal Process.* **69**, 878–891 (2021)
21. W. Yi, L. Chai, Heterogeneous multi-sensor fusion with random finite set multi-object densities. *IEEE Trans. Signal Process.* **69**, 3399–3414 (2021)
22. D. Ciunzo, P.S. Rossi, P.K. Varshney, Distributed detection in wireless sensor networks under multiplicative fading via generalized score tests. *IEEE Internet Things J.* **8**(11), 9059–9071 (2021)
23. T. Li, X. Wang, Y. Liang, Q. Pan, On arithmetic average fusion and its application for distributed multi-Bernoulli multi-target tracking. *IEEE Trans. Signal Process.* **68**, 2883–2896 (2020)
24. T. Li, M. Mallick, Q. Pan, A parallel filtering-communication-based cardinality consensus approach for real-time distributed PHD filtering. *IEEE Sens. J.* **20**(22), 13824–13832 (2020)
25. M. Mallick, K.-C. Chang, S. Arulampalam, Y. Yan, Heterogeneous track-to-track fusion in 3-d usingIRST sensor and air MTI radar. *IEEE Trans. Aerosp. Electron. Sys.* **55**(6), 3062–3079 (2019)
26. X. Cheng, D. Ciunzo, P.S. Rossi, Multibit decentralized detection through fusing smart and dumb sensors based on Rao test. *IEEE Trans. Aerosp. Electron. Sys.* **56**(2), 1391–1405 (2020)
27. D. Ciunzo, S.H. Javadi, A. Mohammadi, P.S. Rossi, Bandwidth-constrained decentralized detection of an unknown vector signal via multisensor fusion. *IEEE Trans. Signal Inf. Process. Over Netw.* **6**, 744–758 (2020)
28. D.A. Castanon, Approximate Dynamic Programming for Sensor Management. In: *Proceedings of the 36th IEEE Conference on Decision and Control* **2**, 1202–1207 (1997)
29. V. Krishnamurthy, B. Wahlberg, *Finite Dimensional Algorithms for Optimal Scheduling of Hidden Markov Model Sensors*. In: 2001 IEEE International Conference on Acoustics, Speech, and Signal Processing. *Proceedings (Cat. No.01CH37221)* **6**, 3973–3976 (2001)
30. J. Evans, V. Krishnamurthy, Optimal sensor scheduling for hidden Markov model state estimation. *Int. J. Control* **74**(18), 1737–1742 (2001)
31. B. Ristic, B.-N. Vo, Sensor control for multi-object state-space estimation using random finite sets. *Automatica* **46**(11), 1812–1818 (2010)
32. B. Ristic, B.-N. Vo, D. Clark, A note on the reward function for PHD filters with sensor control. *IEEE Trans. Aerosp. Electron. Sys.* **47**(2), 1521–1529 (2011)
33. H.G. Hoang, B.T. Vo, Sensor management for multi-target tracking via multi-Bernoulli filtering. *Automatica* **50**, 1135–1142 (2014)
34. H. Cai, Y. Yang, R. Hoseinnezhad, R. Norman, K. Zhang, Multisensor tasking using analytical Rényi divergence in labeled multi-bernoulli filtering. *J. Guidance Control Dyn.* **42**(9), 2078–2085 (2019)
35. H.G. Hoang, B.-N. Vo, B.-T. Vo, R. Mahler, The Cauchy-Schwarz divergence for Poisson point processes. *IEEE Trans. Inf. Theory* **61**(8), 4475–4485 (2015)
36. A.K. Gostar, R. Hoseinnezhad, T. Rathnayake, X. Wang, A. Bab-Hadiashar, Constrained sensor control for labeled multi-Bernoulli filter using Cauchy-Schwarz divergence. *IEEE Signal Process. Lett.* **24**(9), 1313–1317 (2017)
37. M. Beard, B.-T. Vo, B.-N. Vo, S. Arulampalam, Void probabilities and Cauchy-Schwarz divergence for generalized labeled multi-Bernoulli models. *IEEE Trans. Signal Process.* **65**(19), 5047–5061 (2017)
38. A.K. Gostar, R. Hoseinnezhad, A. Bab-Hadiashar, W. Liu, Sensor-management for multitarget filters via minimization of posterior dispersion. *IEEE Trans. Aerosp. Electron. Sys.* **53**(6), 2877–2884 (2017)
39. A.K. Gostar, R. Hoseinnezhad, A. Bab-Hadiashar, Multi-Bernoulli sensor control via minimization of expected estimation errors. *IEEE Trans. Aerosp. Electron. Sys.* **51**(3), 1762–1773 (2015)
40. Y. Zhu, J. Wang, S. Liang, Multi-objective optimization based multi-Bernoulli sensor selection for multi-target tracking. *Sensors* **19**(4), 980 (2019)
41. L. Ma, K. Xue, P. Wang, Multitarget tracking with spatial nonmaximum suppressed sensor selection. *Math. Probl. Eng.* **4**, 1–10 (2015)

42. L. Ma, K. Xue, P. Wang, Distributed multiagent control approach for multitarget tracking. *Math. Probl. Eng.* **1**, 1–10 (2015)
43. Y. Zhu, S. Liang, M. Gong, J. Yan, Decomposed POMDP optimization-based sensor management for multi-target tracking in passive multi-sensor systems. *IEEE Sens. J.* **22**(4), 3565–3578 (2022)
44. R. Mahler, Multitarget sensor management of dispersed mobile sensors, in *Theory and Algorithms for Cooperative Systems*, ed. by D. Grundel, R. Murphey, P.M. Pardalos (World Scientific, Singapore, 2004), pp. 239–310
45. B. Ristic, A. Farina, Target tracking via multi-static Doppler shifts. *IET Radar Sonar Navig.* **7**(5), 508–516 (2013)
46. D. Schuhmacher, B.-T. Vo, B.-N. Vo, A consistent metric for performance evaluation of multi-object filters. *IEEE Trans. Signal Process.* **56**(8), 3447–3457 (2008)

### Publisher's Note

Springer Nature remains neutral with regard to jurisdictional claims in published maps and institutional affiliations.

**Submit your manuscript to a SpringerOpen<sup>®</sup> journal and benefit from:**

- ▶ Convenient online submission
- ▶ Rigorous peer review
- ▶ Open access: articles freely available online
- ▶ High visibility within the field
- ▶ Retaining the copyright to your article

---

Submit your next manuscript at ▶ [springeropen.com](https://www.springeropen.com)

---